promoting access to White Rose research papers

Universities of Leeds, Sheffield and York
http://eprints.whiterose.ac.uk/

This is the author's version of an article published in **International Journal of Hydrogen Energy**

White Rose Research Online URL for this paper:

http://eprints.whiterose.ac.uk/id/eprint/75985

Published article:

Dupont, V, Ross, AB, Hanley, I and Twigg, MV (2007) *Unmixed steam reforming of methane and sunflower oil: A single-reactor process for H-2-rich gas.* International Journal of Hydrogen Energy, 32 (1). 67 - 79. ISSN 0360-3199

http://dx.doi.org/10.1016/j.ijhydene.2006.06.033

White Rose Research Online
eprints@whiterose.ac.uk

Unmixed steam reforming of methane and sunflower oil: A single-reactor process for H_2-rich gas

V. Dupont[a*], A.B. Ross[a], I. Hanley[a], M. V. Twigg[b]

[a]ERRI-SPEME, The University of Leeds, Leeds, LS2 9JT, UK

[b]Johnson Matthey, Catalytic Systems Division, Orchard Road, Royston, SG8 5HE, UK

* corresponding author. V.Dupont@leeds.ac.uk

Paper accepted and published. Full reference:

V. Dupont, A. B. Ross, I. Hanley, and M. V. Twigg, 2007. Unmixed Steam Reforming of Methane and Sunflower Oil: A Single-Reactor Process for H2-rich Gas. International Journal of Hydrogen Energy Volume 32, Issue 1 , January 2007, Pages 67-79

Abstract

Initial tests results are presented for the novel process of hydrogen production called unmixed steam reforming (USR) using methane and sunflower oil fuels. The USR process relies on two mass transfer materials which operate on a two-step cycle: an oxygen transfer material (OTM) which provides the heat necessary for the steam reforming reaction, and a CO_2-sorbent which shifts the water gas reaction yielding a H_2-rich reformate gas. A shortlist of Ni-based OTMs and a natural dolomite were tested during bench-scale investigation and optimisation stages following micro-reactor tests. Under near-isothermal conditions, we show the sequence via which the main reactions occurred. We unexpectedly found that thermal decomposition of the fuel played a

significant role in the early H_2 production concurrent with coking conditions, by causing the OTM to initially reduce. The direct OTM reduction from the fuel via the unmixed combustion reaction then took over to a point where the steam reforming reaction could begin. Most importantly, carbon lay-down (coking) during the fuel/steam flow did not lower gradually the process efficiency, as it was shown to completely oxidise under the cyclic feeds of air and fuel/steam flows of the USR process. Both methane and sunflower oil were shown to be suitable fuels for the USR process.

Keywords: *methane, sunflower oil, steam reforming, unmixed, catalytic, coking*

1. Introduction

1.1. Background

Most western countries are seen dedicating significant research activities in the international effort to realise the transition from a fossil fuel–dominated way of life to a hydrogen economy. For developing countries, the possibilities of leapfrogging to new clean energy technologies such as hydrogen are being explored through dynamic research programs that make the most of their natural resources. The challenge resides in replacing fossil-fuelled transport energy and power generation by renewable hydrogen-powered fuel cells, so that climate change, urban pollution and economic dependency on foreign oil are curbed in the mid and long term. At present, the principal industrial process for converting hydrocarbons into hydrogen gas is catalytic steam

reforming coupled with catalytic partial oxidation (CSR-CPO), the latter adjunct providing the heat necessary for the process which requires temperatures ca. 800°C. Because of the sensitivity of the steam reforming and partial oxidation catalysts to solid carbon formation (coking), this dual catalytic process is restricted to the conversion of light fossil fuels such as natural gas, liquid petroleum gas (LPG) or naphtha, for which suitable catalysts have been developed over the years. Because of this reliance on fossil fuels as feedstock, mass-generation of hydrogen is at the moment a contributor to greenhouse gas emissions and will increasingly be so in the transitional period leading to a H_2 economy. When considering that transportation is the sector that will undergo the fastest growth worldwide in energy consumption within the next ten years, accompanied by a massive increase in high purity H_2-fuelled PEM fuel cells utilisation, novel ways of improving the efficiency of H_2-rich gas reforming processes, as well as widening the range of their hydrocarbon feedstocks is a worthwhile enterprise. Fuels for hydrogen production from biomass provide the most environmentally friendly option. When in addition they are combined with cheap and relatively simple biological processes, the economics and environment-friendly credentials of H_2 production are the most attractive. At present, bio-hydrogen requires types of biomass with very specific characteristics (green algae, or carbohydrates) [1]. Means of converting a wider range of biomass types to hydrogen can be ensured by more costly thermo-chemical treatments like steam reforming of biogas or steam gasification of solid biomass, on condition that these are down-scaleable economically. Even the most popular of bio-hydrogen processes, the dark fermentation of carbohydrates, is optimised to produce hydrogen while producing the by-products acetate and butyrate. The latter are then further processed via

anaerobic digestion to produce a mixture of hydrogen and methane [2]. This bio-methane which is a co-product of bio-hydrogen then becomes a strong candidate for steam reforming.

In [3] and [4], Kumar, Lyon et al. proposed "an alternative process to fire" they termed unmixed combustion, which could be used to provide heat to catalytic endothermic reactions such as steam reforming. In this context, using a single reactor, the process of unmixed steam reforming (USR) produced intermittently a rich H_2 reformate gas, and a separate O_2-depleted air stream containing most of the CO_2 co-product of the steam reforming/water gas shift /catalyst reduction reactions, thereby providing the option for the easy separation and storage of both gas mixtures. In addition the process was claimed to be insensitive to coking and sulphur and therefore diverse fuels could be used. The process could be optimised to run autothermally, i.e. no external heating was required. Finally, it was economical even at small scale (demonstration down to 10kW [4]) because of its heat transfer characteristics, thereby widening the potential the application of USR to distributed power generation from a range of biomass and non-biomass wastes. In [3-4] test results were presented using methane then diesel fuel, the latter with applications to fuelling mobile fuel cells. Later, as GE and the DOE invested $5M in this technology, for larger scale power generation, the terms 'autothermal cyclic reforming' [5] and unmixed fuel processing (UFP) were also employed [6-7].

This paper aims to present results of a project undertaken to test the principle of unmixed steam reforming using a renewable fuel with coking tendencies such as vegetable oil. But on the way to this aim, so little was in public knowledge about the reaction chemistry involved in the unmixed steam reforming process that a significant portion of this study was conducted using the simpler gas methane as a model, while concentrating on isothermal reactor conditions. Thus the results in

this paper were obtained mostly using methane fuel and to a lower extent, sunflower oil. The process requires the use of two 'Transfer Materials', one for oxygen and another for carbon dioxide (a CO_2-sorbent). Following a thermodynamic assessment of the process, the right oxygen transfer materials (or OTMs) and CO_2-sorbents were identified by carrying out redox and CO_2-sorption cycle tests in a micro-reactor. The transient operation of the process at bench scale and near-isothermal conditions was then conducted, with the associated elemental balances providing the sequence of the basic chemical reactions of the USR process.

1.2. Principle of Unmixed Steam Reforming (USR)

1.2.1. Under airflow (AF):

In Lyon et al.'s theory [3-4], under airflow, the oxidation of a metal is used to provide heat to a reactor housing an endothermic reaction. The subsequent reduction of the metal oxide by the fuel or a fuel decomposition by-product causes its 'unmixed' combustion, i.e. its combustion without direct contact with the oxygen-containing stream, while the still hot reactor bed allows the endothermic reaction to proceed. In our case this was the reforming of a hydrocarbon (CH_4) and subsequently, of a biofuel (sunflower oil) with steam to produce H_2, CO and CO_2. Oxygen transfer material candidates for unmixed combustion such as copper or iron with low melting points were disregarded in favour of nickel, which could withstand the higher temperatures required by steam reforming (ca. 800°C). Note that 'OTM' was employed in [7] whereas earlier work on USR [3-4] used the term of 'oxygen mass transfer catalyst'. As the latter terminology

could confuse the reader into conventional catalysis thinking, i.e. that such materials do not affect thermodynamics of reactions, we have adopted here the more correct nomenclature of 'oxygen transfer material', which does. The process consisted of alternated feedstreams of airflow (henceforth termed 'AF') with fuel/steam flow ('FF') over a fixed bed of mixed OTM and CO_2-sorbent in granulated form. The OTM undergoes the redox reactions $Ni + 0.5\ O_2 \rightarrow NiO$ and $Fuel + NiO \rightarrow CO_2 + Ni + H_2O$ (the latter is termed the unmixed combustion reaction) under AF and FF respectively. The Ni support material, mainly alumina, was assumed to be inert. Using thermodynamics equilibrium calculations, we calculated that the oxidation of Ni would release 2.4×10^5 J/mol of Ni reactant at around 800°C ($\Delta H = -2.4 \times 10^5$J/mol Ni) with 100% conversion. In the Lyon et al. theory [4], when a CO_2-sorbent ('MO') is present in the reactor, a solid carbonate (MCO_3) is formed under fuel/steam flow by binding the CO_2 produced through steam reforming, unmixed combustion or water gas shift. The carbonation reaction works as a dry-H_2 content enhancer by shifting the equilibrium of the water gas reaction. Then, under the subsequent airflow, the carbonate 'MCO_3' decomposes thermally through the reaction $MCO_3 \rightarrow MO + CO_2$. The reaction acts as a CO_2-sorbent regenerator within the reformer, as opposed to current sorbent-enhanced steam reforming processes which require a separate regenerator. Depending on the chosen element 'M', different temperature ranges are accessible for the CO_2-sorption process, and the enthalpies of reaction also differ, affecting the autothermal requirements of the USR process. Thus initially the reactions under AF were assumed to be:

(AF1) $Ni_{(S)} + 0.5\ O_2 \rightarrow NiO_{(S)}$ *-OTM oxidation, exothermic*

(AF2) $MCO_{3(S)} \rightarrow MO_{(S)} + CO_2$, where M is Ca or Mg. *thermal decomposition of CO_2-sorbent (or sorbent regeneration), endothermic*

To which the reactions were later added as a result of the present study:

(AF3) $C_{(S)} + O_2 \rightarrow CO_2$, *complete oxidation of carbon, exothermic*.

(AF4): $C_{(S)} + 0.5O_2 \rightarrow CO$, *partial oxidation of carbon, exothermic*.

The overall enthalpic balance of the airflow sequence should be exothermic, storing and then releasing sufficient heat during the following fuel/steam flow globally endothermic reaction sequence. The cycles are then repeated.

1.2.2. Under fuel/steam flow (FF)

Under fuel/steam flow, the reactions postulated in [4] were those of: steam reforming, OTM reduction, and sorbent carbonation. No path or sequence was specified and we speculated that the reactions were simultaneous and initially as follows:

(FF1) $C_nH_mO_k + (n - k)\ H_2O \Rightarrow n\ CO + (n + m/2 - k)\ H_2$ *Steam reforming (endothermic).*

For methane, n = 1, m = 4, k = 0, for sunflower oil, typically n = 18, m = 34.4, k = 2.1.

(FF2) $CO + H_2O \Leftrightarrow H_2 + CO_2$ *Water gas shift* (exothermic)

(FF3) $C_nH_mO_k + (2n + m/2 - k)\ NiO_{(S)} \Rightarrow nCO_2 + m/2\ H_2O + (2n + m/2 - k)\ Ni_{(S)}$ *OTM reduction* (*Unmixed combustion of fuel, endothermic for methane).*

Steam reforming and water gas shift occur alongside one another, therefore, when no CO_2-sorbent is used, there is a maximum yield of H_2 (ca. 70% dry H_2) determined by thermodynamic limitations. Both steam reforming and the OTM's reduction are fuel consumers under the same flow. The mechanism by which the two reactions proceed in practice was not covered in previous publications on the USR process [3-7], and was therefore addressed in our investigation. If a

CO_2-sorbent was present as a H_2 yield enhancer, then the carbonation reaction below also occurred during the FF step.

(FF4) $MO_{(S)} + CO_2 \Rightarrow MCO_{3(S)}$, where M could be Ca, Mg, Ba or more complex groups. *Carbonation of MO, (exothermic).*

Globally, the above reactions under FF were summarised by

$(MO_{(S)} + NiO_{(S)}) + fuel + H_2O \Rightarrow (MCO_{3(S)} + Ni_{(S)}) + little\ (CO, CO_2, H_2O, O_2) + ca.80\%$ H_2.(*endothermic*).

The (S) subscript indicates a species in solid phase, but in the text that follows we will no longer use the subscripts except for $C_{(S)}$.

We went on to find as a result of this study that additional reactions needed to be taken into account. These were FF5 and to a lower extent, FF6.

(FF5): $CH_4 \rightarrow C_{(S)} + 2H_2$, *thermal decomposition of methane, coking (endothermic).*

(FF6): $2CO \leftrightarrow C_{(S)} + CO_2$ *Boudouard reaction (exothermic) and its reverse*.

2. Results and Discussion

The unmixed steam reforming process was shown in [4] to operate in a stable manner using diesel fuel and it was therefore inferred that the process was insensitive to coking. There was however no mention of how much coking, if any, was part of the process. One aspect of the study was to determine in a first stage what the thermodynamics limitations of these reactions were by using modelling, which forms section 2.1 of this paper. In section 2.2., we summarise results

from micro reactor tests aimed at identifying the most suitable OTM and CO_2-sorbents. A description of the bench scale set up follows in 2.3. Three OTMs were subsequently investigated in the bench scale process under near-isothermal conditions (800°C) and in the absence of CO_2-sorbent, in order to determine the chemical mechanisms underlying the fuel/steam step and the airflow step, for which results are presented in 2.4. Methane and vegetable oil are considered in turn as the fuel in this section. In the final section 2.5, initial results from near isothermal tests at bench scale using methane and in the presence of a CO_2-sorbent are presented.

2.1. Determining theoretical autothermal conditions using thermodynamics modelling

Thermodynamics equilibrium calculations were carried out with the code PSR from CHEMKIN [8] to assess the validity of the USR principle, and provide relative amounts of reactants to be used.. Table 1 is an illustration of the input conditions and outputs for theoretical autothermal operation of the reforming of methane. The unmixed process is compared with the CSR/CPO conventional process for the steam/methane molar ratio of 2. Calculations are performed on the USR process firstly in the absence of CO_2-sorbent (first two rows), then using a CaO-based CO_2-sorbent which used the $CaO + CO_2 \Leftrightarrow CaCO_3$ cycle (3^{rd} and 4^{th} rows). The reactant fractions for autothermal behaviour were calculated based on a balance of enthalpies of the reactions proposed earlier under each flow. In all the calculations summarised in Table 1, the formation of solid carbon was not allowed, simulating an optimal operation, but many other calculations (not shown

here) were carried out with possibility of $C_{(S)}$ in the products, i.e. carbon graphite product under FF and reactant under AF.

In the absence of CO_2-sorbent, the USR process under fuel/steam flow 'FF', alternated with airflow 'AF', (top two rows) was predicted with the reactant mol fractions as defined in the third column. It yielded equilibrium outputs of dry hydrogen content of 70.9%, with a production efficiency of 0.71 moles of H_2 produced per mol of 2H input into the process by the combination of methane and water. Assuming an adiabatic process, this corresponded to a heat release (ΔH) of 2.4×10^5 J/mol of Ni under airflow, and a heat consumption of the same magnitude under fuel flow (8^{th} column), demonstrating the unexpected potential for autothermal operation in the absence of CO_2 sorbent. By comparison, the conventional CSR/CPO operating autothermally, produced the same output on a same steam to carbon ratio basis (last row).

Introducing the CaO-based CO_2-sorbent in the thermodynamics calculations and performing the runs with a USR reactor temperature of 717°C under fuel flow yielded slightly disappointing results in terms of dry hydrogen yield (75.5%). For such a run, autothermality was established on the basis of 1.8×10^5 J/mol of Ni transferred from the AF step to the FF step. This lower-than-expected dry H_2 yield is brought about because in the 600-800°C range, the predicted theoretical equilibrium efficiency of CaO carbonation drops very significantly. Table 1 shows an efficiency of carbonation (CaO conv.) of only 55% at 717°C. It then drops to just 20% at 800°C and is accompanied by a drop of dry H_2 content to 72% and an increase in heat demand to 2.3×10^5 J/mol of NiO under FF, which is then no longer matched by the exothermicity of the AF step. We shall see in the results section that experiments on CaO carbonation exhibit a high efficiency up

to 830°C. Thermodynamic equilibrium modelling can therefore be used for trends rather than absolute values. Nevertheless, the conditions for autothermal behaviour should in theory be extremely sensitive to the carbonation efficiency and thus to the maximum temperature allowable under FF. With a CaO-based CO_2-sorbent assumed in the reactor, the H_2 production efficiency calculated at 717 °C using thermodynamics modelling was slightly higher (0.81 mol of H_2/mol of 2H input) than without the sorbent at 800°C. In fact, Lyon and Cole explain in [4] that the temperature fluctuations and profile in the reactor make carbonation possible. Increased gas pressure under FF also improves the carbonation efficiency and the enthalpy balance by reducing the heat demand, although in our calculations, the theoretical percent fuel conversion efficiency also dropped to the lower nineties as a result, which we deemed undesirable. This is why the rest of the work was carried out at atmospheric pressure.

If one allowed for carbon graphite formation in the process, several effects were found. From equilibrium calculations, at 800°C, in the absence of OTM, 18% of the methane would be expected to convert to carbon at equilibrium. There is a significant enthalpic effect as carbon lay-down during the fuel flow reduces the heat demand under FF but requires that the carbon oxidise completely during AF. With a carbon oxidation enthalpy of -3.88×10^5 J/mol of C at 800°C, this is more exothermic than the Ni oxidation reaction (-2.44×10^5 J/mol of Ni). Thus if carbon graphite were formed in significant amounts under fuel flow, the energy demands and process outputs of the unmixed process could be construed as fundamentally different than anticipated. In reality, carbon formation on nickel materials during the thermal decomposition of methane or steam reforming conditions exhibits different thermodynamic properties and kinetics than carbon

graphite [9], this should reduce somewhat the large enthalpic differences expected between the USR with and without carbon formation.

2.2. Oxygen transfer materials (OTMs) and CO_2-sorbents testing in a micro-reactor

In the conventional CSR/CPO process, oxidised Ni-catalysts are known to have much less activity than when reduced. Before steam reforming begins, a thorough reduction treatment of the catalyst needs to be carried out. Most steam-reforming catalysts found in industry are Ni based, impregnated on various ceramic supports, with additional minor components with a coking-resistant role [10]. In [4], results of USR tests are presented using similar materials as the chosen OTMs. Similarly, we chose a number of supported Ni materials from Johnson Matthey (catalysts from the steam reforming or methanation groups) to be tested in the USR conditions as potential oxygen transfer materials for our tests. We expected that larger Ni contents in the OTM would cause larger heat release rates under airflow, and would ease the conditions for autothermal behaviour. However issues of thermal stability as well as transient behaviour of the OTM were to be considered as it was subjected to cyclic temperature profiles under the redox conditions of the alternated air and fuel/steam flows. Larger Ni content OTMs were expected to be less thermally stable. We also assumed that, as described in [3-4] because the fuel and steam met over a hot oxidised material, the steam reforming reaction would not be catalytic. The assumption was going to be proved wrong from our bench scale isothermal tests.

2.2.1. Evaluation of Oxygen Transfer Materials

A fast Ni oxidation rate is desirable for the unmixed process to rely on an airflow step as short as possible, and to produce hydrogen for the largest period of the cycle under fuel flow. More importantly, a Ni oxidation time shorter than the duration of H_2 production would ensure that H_2 is produced continuously when two reactors are run in parallel and out of step. Given the importance of this aspect in the USR process, six Ni-based OTMs with different Ni contents and termed alphabetically 'A' to 'F' were identified and tested using the methodology described in our first publication on the project [11], which subjected the materials to repeated cyclic air/methane flows. This is summarised in Table 2.

All OTMs tested by thermogravimetric analysis were thermally stable except 'D'. The maximum Ni conversion rate to NiO for oxidation with excess air is listed in Table 2 along with maximum rate of oxygen conversion. Surprisingly there is a lack of correlation between the OTM's Ni content and the maximum rate of Ni oxidation. The tests were primarily to assess the redox ability of the materials, which all of them ended up exhibiting. The larger maximum rate of oxygen conversion indicated that Ni oxidation was not the only reaction competing for oxygen. In fact, as the OTM was subjected to reduction under methane flow and oxidation under airflow, the reduction reaction was shown to occur via H_2 as evidenced by small amounts of evolved CO_2 and CO (not shown here). It would therefore seem that the unmixed combustion reaction FF3 occurs preferably through H_2 fuel over CH_4 fuel. The resulting solid carbon then burned during the subsequent airflow. This feature was to become a prominent aspect in the bench scale USR process.

2.2.2. Evaluation of CO_2 sorbents

Our thermodynamic calculations indicated that among MgO, CaO, BaO and SrO as CO_2-sorbent candidates, the properties of CaO were better suited to the USR conditions. It was predicted to still bind CO_2 at 800°C, albeit with the less than ideal theoretical efficiency of 50%, based on thermodynamic calculations. At the time of the project, a new generation of low temperature CO_2-sorbent materials was appearing in the literature, and it was felt that tests had to be carried out to check the suitability of a number of such sorbents under the cycling conditions of unmixed steam reforming. Another methodology using the same micro-reactor was established to test various conventional and novel CO_2-sorbents and is described in detail in [11, 13]. This methodology was to address the CO_2 sorption capacity as well as how this was maintained under sorption/regeneration cycles simulating the alternated FF and AF steps of USR. Reference [11] lists the CO_2-sorption capacity (in g of CO_2/kg of sorbent) for each of the 13 materials tested (some bought off-the shelf, some produced in-house). Tests under repeated carbonation/thermal decomposition cycling indicated that a Spanish dolomite, originating from Sierra de Arcos, and with a composition by weight of 29.4% CaO, 19.3% MgO, 3.8% SiO_2, 1.7% Al_2O_3, 0.6% Fe_2O_3, < 0.1% K_2O, with balance CO_2), together with $CaCO_3$ manufactured in-house from acetate, were the most stable of the short-listed CO_2-sorbents.

2.3. Experimental set-up of the bench scale USR process

Figure 1 shows a diagram of the USR bench scale process set up. Reactant gases were controlled by three mass flow controllers for nitrogen, methane and air followed by three solenoid valves operated in sequence. The liquid feeds of water and vegetable oil were regulated by two actuated

valves switching between the AF and FF. All valves were centrally controlled by a sequence generator. When the unit was not operating (not cycling), a third valve allowed flushing of the assembly with nitrogen.

The product gases were cooled using a water-cooled condenser before entering a water trap (ice bath), followed by a chemical water trap (silica gel). The dry gaseous products CO/CO_2, CH_4, H_2 and O_2 were fed through a series of on-line analysers from ABB and data-logged. The gas reaching the analysers was dry and at room temperature. For safety reasons, the entire gas product stream was diluted with air and N_2 and disposed of by flowing it over resistively-heated platinum gauze within an enclosure, where its combustible components burned relying on catalytic combustion. Two relief valves were situated before and after the reactor to maintain the reactor pressure below 2 bar. Pressure and temperature readings were measured at various points in the rig as described in Fig. 1. The reactor had an internal volume of 80 cm^3. It contained a combination of an OTM chosen from our microreactor study in (2.2.1) and in the final tests, a mixture of OTM and a natural dolomite (Sierra de Arcos, Spain), in ground pellets form of approximately 1-2 mm size, preceded and succeeded by two plugs of inert alumina particles. We report here experiments where either 80 or 40 g of OTM were used. The reactor was heated externally by a coiled 1 kW tubing heater which was actuated in an 'on-off' control feedback loop using the middle-reactor thermocouple as the measuring element, and a reference temperature that could be set in the range 600-800°C. The heating element was first clad with K wool then surrounded by an alumina casing itself enclosed in a stainless steel casing. For the experiments reported here, the middle-reactor temperature was set at 800°C with the on-off controlled heating. Figure 2 shows typical temperature histories obtained under FF and AF (with

a short purge of N_2 flow in between). It can be seen that the reactor core surrounding the OTM and the sorbent materials remained at a constant temperature close to 800°C during the globally endothermic FF step, while its downstream and upstream extremities, which corresponded to the plugs of alumina particles, were significantly cooler. The AF step, which the oxidations of the OTM and carbon make globally exothermic, exhibited a sharp peak to ca. 1100°C which then returned back to 800°C over the duration of the AF.

2.4. Investigating the process: near-isothermal tests in absence of CO_2-sorbent

In this section, the FF step under CH_4 fuel is examined first, followed by a short section on the AF step (which showed similar behaviour under both CH_4 and sunflower fuel flows), and finally results on the FF step under sunflower fuel flow are discussed.

Methane fuel was first investigated in order to find out some aspects not covered in the literature about the unmixed steam reforming process: i.e. the mechanism by which the steam reforming and the NiO reduction reactions occurred, whether carbon formation took place and how sensitive the process was to it. Detailed elemental balances were carried out during cycled AF step and N_2-diluted FF step, and in the absence of CO_2-sorbent to address these issues. Both these conditions in conjunction with using the simple fuel CH_4 were necessary measures permitting closure of the elemental balances on the basis of the range of our on-line dry gas measurements. In these balances, we assumed that the only carbon-containing products of the conversion of the CH_4 fuel were CO, CO_2, and $C_{(S)}$. The latter was verified by sporadic off-line GC analysis of the reformate gas for detection of higher carbon hydrocarbons, which revealed negligible amounts.

Under sunflower oil flow, CH_4 was included as a product in the balances, accordingly to our measurements.

2.4.1. Investigation of the reaction mechanism under the CH_4/Steam flow step

We show in Table 3 examples illustrating how three of the OTMs tested in the microreactor performed differently in the USR process when using a middle-reactor temperature set at 800°C with the steam/CH_4 ratio of 1.8 under two flows of methane. The steam/CH_4 ratio of 1.8 had previously been identified in a range of ratios from 1 to 3 as the ratio yielding the highest dry H_2 content in the reformate gas.

It can be seen from Table 3 that all three OTMs presented a 'dead time', i.e. an initial period under FF where no H_2 evolved from the reactor. The OTM 'A', which had a medium Ni content, exhibited the shortest dead time of the three OTMs investigated at bench scale. The dead time was seen to decrease for the larger methane flow rate. Figures 3a-b plot the histories of CH_4 and H_2O conversions for the whole duration of the fuel/steam flow (600 s) for the OTM'A'. Figures termed 'a' correspond to a CH_4 flow of 152 sccm, or 1.13×10^{-4} mol s^{-1}. For figures 'b', the flow of CH_4 was 400 sccm (or 3×10^{-4} mol s^{-1}). The histories of selectivity for CO, CO_2 and $C_{(S)}$ are plotted in Figs 4a-b. The dry percent H_2 content (corrected for zero N_2 content) can be seen in Figs 5a-b. The histories of NiO conversion rate together with the NiO % conversion are shown in Figs.6a-b. The curves were all constructed from the outputs of the detailed elemental balances, and exhibited similar profiles for the other OTMs tested. In the discussion that follows, we identify the sequence of reactions at work during the fuel/steam feed by examining the product

gas composition with time as well as the rates of OTM redox and carbon formation determined by elemental balances.

A very short first stage of approximately 30 s duration can be identified from Figs. 3a-6a, whereby CH_4 was consumed while $C_{(S)}$, H_2, reduced Ni, and H_2O (evidenced by a negative H_2O conversion) were formed. Over this period $C_{(S)}$ formation was constant while H_2 conversion efficiency was zero. The absence of CO_2 in this initial stage indicated that reaction (FF3), i.e. the reduction of NiO to Ni directly by CH_4, was inactive during this initial stage of the FF step. The production of H_2O rather than its consumption, as well as the absence of CO, were evidence that steam reforming and water gas shift were dormant, and thus that the initial consumption of methane was via thermal decomposition only. This justified considering reaction (FF5) $CH_4 \rightarrow C_{(S)} + 2H_2$ as a player in the USR mechanism in its own right. A second short stage followed (until 100 s), where the sharp decline of H_2 down to zero was concurrent with an equally sharp increase in NiO reduction rate and CO_2 formation. This indicated the NiO was being reduced by all the H_2 product of reaction (FF5), as well by methane itself, through reaction (FF3). Note that with our definition of reaction (FF3), hydrogen, CO and carbon could act as the OTM reductant. The extent of reaction (FF5), which we had to introduce at this point, was not considered significant in [3-4] and was only revealed here by the detailed elemental balances to which we subjected the methane/steam flow step. The reduction of the Ni-based OTM by H_2 was mass transfer limited by the flow of CH_4 as indicated by a conversion of the latter to nearly 100%.

Comparing these two initial stages to the equivalent period in Figs.3-6b under an increased methane flow indicated that there was earlier formation of CO_2 and CO, as well as H_2O conversion, hinting at an earlier steam reforming activity. The evolution of $C_{(S)}$ soon followed by

CO_2 and the sharp decline of H_2 suggested that the thermal decomposition of methane (FF5), and the resulting reduction of NiO with H_2 and CH_4 were nearly simultaneous. In addition (FF5) was sufficient to generate hydrogen in excess of the NiO reduction demand so that H_2 was seen to evolve from the reactor from the start and the dead time was greatly reduced. A comparison of the rates of NiO reduction between Figs 6a and 6b indicated that the peak rate increased significantly with the flow of reactant methane.

A third stage in all the figures was identified, whereby gradually for both low and high fuel flows, the steam reforming reaction (FF1) grew from non existent to a plateau of steady activity, as evidenced by steam being consumed (H_2O conversion becomes positive) and CO production taking off, while CO_2 and $C_{(S)}$ reach a minimum (see columns 2-6 of table 3 for average values). We found that steam reforming kick-started once a significant portion of the Ni present in the OTM had reduced Ni, typically 10-15% of the total Ni in the reactor (Figs. 6a-b). At this point the NiO reduction rate decreased sharply and resumed a constant value as it competed for fuel with the steam reforming reaction and methane thermal decomposition. Note that as the Ni material did not flow in or out of the reactor, its conversion from NiO to Ni during the FF step increased steadily from zero to a maximum percent based on the total number of moles of Ni present in the reactor. One should not expect 100% conversion as it would mean that all the Ni was available for heterogeneous solid-gas reaction. The efficiency of the steam reforming reaction was reflected in the value of fuel conversion (ca. 99%) and that of steam (variable between 37-51%) given in the 5^{th} column of Table 3. These separate efficiencies were then combined in a single value of H_2 production efficiency in the penultimate column of table 3, and is based on an average taken in the period of established constant steam reforming. It varied

between 0.66 and 0.76, with the OTMs ‘A’ and ‘B’ exhibiting the highest average efficiencies with the lower flow of CH_4. The last column in table 3 lists a ‘final H_2 efficiency’ which is significantly lower than the average listed in the column before it. This final efficiency is the total hydrogen conversion from the combined methane and water inflows since the FF step began until it ended. Thus it is significantly affected by the dead time ratio. Decreasing dead time would increase the final efficiency, as would the duration of the FF step. Where there was co-evolution of $C_{(S)}$, CO and CO_2, we can expect that the Boudouard reaction to be in equilibrium with its reverse (FF6: $2CO \leftarrow C_{(S)} + CO_2$). It can be seen from Table 3 that a low fuel flow favoured higher steam conversions for OTMs ‘A’ and ‘B’, but that the dead time became prohibitively long. This was because the fully converted methane flow was limiting the reduction of the NiO, which in turn delayed the onset of steam reforming. Higher methane flows therefore seemed more desirable over the high average steam conversions obtained under the lower FF flows once steam reforming got established. This conclusion is best supported by the values obtained for the final H_2 efficiency, which, on the basis of equal FF durations of 600 s for the three OTMs studied, were larger under the higher CH_4 flow, with a maximum found for OTM ‘A’. Little could be gained from a comparison between OTMs of the average dry % H_2 (corrected for zero N_2) given in the third column from the right of table 3. Indeed values between 75 and 76% were obtained in all the cases once steam reforming was established to the exception of OTM ‘C’ (72.8%) at the lower CH_4 flow rate. This is notably higher than the 70.9 % predicted by the thermodynamic equilibrium calculations of Table 1 for a steam to carbon ratio of 2, which assumed no $C_{(S)}$ formation. Thus, unexpectedly, by allowing some $C_{(S)}$ formation as reflected by values between 5.4 and 13.8% for C(S) selectivity shown in table 3, the USR process produced a

richer dry H_2 content in the reformate gas even in the absence of CO_2 sorbent. Such an unexpected advantage of the USR process is unfortunately mitigated by the presence of the newly discovered 'dead time'. However, we anticipate that the dead time could altogether be eliminated from the FF step. This could be achieved by introducing an intermediate fuel-only feed step whose sole role would be to produce H_2 via thermal decomposition in excess of the NiO reduction demand. The inclusion of such an intermediate step is implied in [7], which reports on later work by the GE team, although the reason for this additional step compared to the earlier work on unmixed steam reforming [3-4] was not explicit. It might have seemed obvious to include this extra step from the start in the process, but the reader needs to remember that in the original USR process as described in [3-4], the Ni material was not intended to be used as a catalyst for steam reforming but only as an oxygen transfer material, which offered the advantage of the process' insensitivity to catalyst poisons. We show through this study that the bed material needs to act as both OTM and steam reforming catalyst in order to take full advantage of the water reactant. As a result, some of its claims of insensitivity to poisons might be compromised. Certainly the issue of sulphur presence in the fuel will need to be closely monitored in future studies. In the case of using sulphur containing fuels, we should also be aware of the potential dual role of the sorbent in binding CO_2 as well as sulphur species.

2.4.2. Investigation of the reaction mechanism under the airflow step

Figures 7 shows the histories of oxygen conversion, Ni and $C_{(S)}$ oxidation rates for the OTM 'A' under airflow. This step followed a FF step that had used vegetable oil (steam:C ratio of 1.8, on 80 g of OTM, at temperatures 700-1100°C, 1200 sccm of air for 575 s). The histories of the

selectivity to the oxygen-containing products CO, CO_2 and NiO can be seen in Fig. 8. The data used in these figures is also representative of what was obtained under repeated cycles under the same conditions.

Figure 7 shows that the carbon oxidation rate was initially 5-7 times larger than the rate of Ni oxidation, corroborating the significant role played by solid carbon deposits during both AF and FF phases of the USR process. The higher carbon oxidation rate implied that the outer surface of the OTM granules was partially coated with carbon. Also, the conditions of oxidation were limited by the flow of oxygen in these runs, as evidenced by the complete conversion of O_2 over the first 240 s. As the OTM initially covered by carbon gradually became exposed, the Ni oxidation rate increased through reaction AF1, while that of carbon decreased. Figure 8 indicates that the oxidation of the solid carbon initially produced similar amounts of CO and CO_2 through reactions AF3 and AF4, which is consistent with competition for oxygen by the OTM and thus incomplete carbon combustion. This might be exacerbated by the reverse Boudouard reaction. CO_2 selectivity is then seen to increase while NiO became the main oxygen-containing product (peak of 80% selectivity). Oxygen overall conversion subsequently decreased, evidencing that most available Ni sites had oxidised while a little carbon was still present. At this point, the remaining carbon burned in excess of oxygen, giving off CO_2.

Results for an AF following a methane fuel/steam step on the same OTM are not shown here, but as for the sunflower oil tests, indicated that the $C_{(S)}$ and Ni oxidation reactions competed for the same oxygen and that their respective rates were in relation to the extent of coking undergone during the previous FF step and to the availability of oxygen. Carbon oxidation under air feed following a methane/steam feed was however in much smaller proportions as for a sunflower oil-

steam feed, due to the lower amount of carbon accumulated. Ni oxidation ended typically when 15-40% of the total Ni present in the reactor had converted, indicating that the remaining nickel in the porous bed material was unavailable for reaction.

2.4.3 Isothermal tests under sunflower oil-steam step with N_2 dilution

These were carried out using downward reactant inflows in an earlier configuration of the bench scale set up. Finding the optimum steam: carbon ratio was the first task, and this was found at 1.8, as in the methane tests. A flow of sunflower oil of 0.575 l/min (3.1×10^{-5} mol/s) was used, corresponding to 5.58×10^{-4} mol of C /s or 5.33×10^{-4} mol of 2H /s. The higher of the two CH_4 fuel flows shown in table 3 had corresponded to 3×10^{-4} mol of C /s or 6×10^{-4} mol of 2H /s. The fuel-hydrogen inflow was therefore similar under the sunflower oil test and the higher methane flow tests of section 2.4.1.

Results for a sunflower oil test and the OTM 'A' are reported in Table 4. At just 32%, the steam conversion shows potential for improvement, the $C_{(S)}$ selectivity of 39.9 % was very high compared to the tests with CH_4, and should also be lowered in future optimisation tests. This might be achieved as a result of the reactor improvements such as upward inflows allowing for better reactant mixing. An additional feature of using sunflower oil as the fuel, was that methane was present in the reformate gas (15.5% of carbon products) and thus showed potential for further H_2 production. As with the methane tests, a period of 'dead time' of 100 s (up to 1/4 of the 400 s duration of the FF step), was dedicated to the thermal decomposition of fuel and to its resulting reduction of the OTM. This was similar to the 100s dead time found with the larger CH_4 flow feed (previous section), indicating that the fuel-hydrogen feed rate determines the dead time

for both fuels tested. The larger mass of OTM in the sunflower oil fuel experiments (80 g) compared to those with methane (40 g) affected the % OTM reduction for which steam reforming began, i.e. 8%, indicating a similar molar amount of reduced Ni in the reactor to those of the methane tests. A major drawback of using sunflower oil is the resulting low average H_2 conversion efficiency (0.44) once steam reforming was established. The low water conversion and the large coking tendency of the sunflower oil were no doubt responsible for this rather poor result. Despite the much more significant coking of this sunflower oil test, the AF step was able to fully oxidise the carbon deposits and thus maintain the efficiency from cycle to cycle. This feature remains a significant advantage which supports the claim of fuel flexibility for the USR process.

2.5. *Isothermal tests with methane, in the presence of a CO_2-sorbent and lack of N_2 dilution*

These tests were carried out in the absence of N_2 dilution (which formerly allowed our elemental balances) and the outputs of the reactor were therefore analysed from unprocessed dry gas data. Results for these tests can be seen in [12-13]. The dry H_2 content during FF steps at 600 and 650 °C using a steam to methane molar ratio of 4, over 66g of the OTM'A' and 21 g of natural dolomite (Sierra de Arcos, Spain) is shown in Figure 9. The dolomite had been identified as one of the most suitable for the USR process during our micro reactor tests (2.2.2) and had been used in a previous study [14]. The dry H_2 content for the run at 600 °C reached above 90% for more than 50% of the duration of the FF, and even peaked at 93%. This dropped to just 75% dry H_2 for

75% of the duration of the run at 650 °C, similarly to the results of Table 3 for tests without sorbent, hinting at little carbonation activity at this temperature. It is widely accepted from the literature, as in for instance [15], that the thermal decomposition of dolomite involves either one or two steps depending on the partial pressure of CO_2. These are:

One- step: $CaMg(CO_3)_2 \rightarrow CaO + MgO + 2CO_2$, which occurs at low pressures in the range [627-677]°C, and

Two- steps: (i) $CaMg(CO_3)_2 \rightarrow CaCO_3 + MgO + CO_2$ at pressures of CO_2 higher than 0.031 atm and beginning at about 687°C. This increases to 897°C at 1 atm, followed by (ii) $CaCO_3 \rightarrow CaO + CO_2$, which begins at around 930°C under pure CO_2 atmosphere [16]. Figure 10 shows the mass loss of the dolomite used in the present study when exposed to thermal decomposition (calcinations) in a TGA under 50 ml/min CO_2 flow with a heating rate of 10°C/min (termed 'calc.1' in Fig. 10). It is followed by mass gain under carbonation (cooling mode of TGA). A second curve (calc.2) of mass gain under a calcination run carried out immediately following the carbonation under the same conditions as the initial calcination is also shown in Fig. 10. The conditions were deliberately chosen as those in [16], where a number of mineral sorbents and in particular a Greek dolomitic rock with 98% dolomite content had been tested. The results obtained here showed very a similar behaviour in the TGA experiment, thereby showing the sorbent material chosen in this study was not out of the ordinary. This consisted of the two-steps thermal decomposition described earlier and obtained for the first calcination run. Two temperature ranges of decomposition were visible: when MgO and CO_2 evolved, between 600 and 780°C, and when CaO and CO_2 evolved, between 930 and 940°C. During the cooling run,

carbonation of the CaO began below 880°C, where most of the mass gain due to formation of $CaCO_3$ was achieved below 860°C. As in [16], the MgO did not recarbonate under cooling as evidenced by the final mass loss of 66% and the absence of a second stage in mass gain. The decomposition of the resulting $CaCO_3$ under the second heating run occurred at a slightly lower temperature (915°C instead of 930°C). It is generally accepted that temperatures of thermal decomposition and of carbonation of sorbent materials vary with parameters such as the gases presents, their partial pressure, the material porous structure, and to a lower extent the TGA experimental parameters. We show in [12-13] that the partial pressure of CO_2 under the 600°C test was for most of the feed duration under 0.03 atm, which would have caused a one-step thermal decomposition at around 680°C rather than the two-steps decomposition obtained under the pure CO_2 atmosphere of the TGA experiments. This could partially explain our lack of carbonation at 650°C in the bench scale experiment. Several effects could in addition have been at work at 650°C and not at 600°C which could have caused a lower carbonation activity, involving the state of the CO_2 sorbent material at the two temperatures and their previous histories under air flow. Higher sintering of the sorbent material, in particular the MgO would be expected at the peak temperatures reached under air flow following the 650°C methane-steam feed, this would have the effect of blocking sorbent pores. Given that detailed elemental balances are unavailable when operating without N_2 dilution and in the presence of CO_2 sorbent, it is difficult to assess whether carbon coverage could have been responsible. Leaving this matter for future studies, we can nevertheless concur with [3-4] that the process is highly sensitive to the carbonation temperature.

3. Conclusions

A number of Ni-based oxygen transfer materials (OTMs) and CO_2-sorbents were identified through micro-reactor tests as potential candidates for the fixed-bed unmixed steam reforming (USR) reactor which operates under cyclic flows of air and of fuel/steam mix. Nearly all OTMs and one CO_2-sorbent (Sierra de Arcos Spanish dolomite) out of thirteen tested showed to be suitable for the subsequent bench scale tests. Experiments at bench-scale using methane and sunflower oil refined a shortlist of three OTMs to a best-performing commercial material containing 27.5wt% Ni with regards to speed of reduction under fuel/steam flow. Investigating the chemical mechanisms underlying the USR process revealed that carbon formation under fuel/steam flow and its subsequent oxidation under airflow played a significant role. Under methane flow, the hydrogen production routes were ensured mainly by steam reforming, but also to a lower extent and unexpectedly by the thermal decomposition of the fuel to solid carbon and hydrogen in the conditions tested (ca. 800°C and three OTMs studied). One effect of the fuel thermal decomposition was that the dry H_2 content of the reformate gas neared 75% even in the absence of CO_2 sorbent, when 70.9% was the maximum expected in the absence of carbon formation. In addition, steam reforming only proceeded once sufficient NiO from the OTM created previously under airflow had reduced back to Ni, typically of the order of 10-15% of the total Ni present in the reactor for a 40 g OTM batch. This made the rate of NiO reduction a most important parameter in the overall process efficiency. Under conditions of low fuel/steam flow, an initial ‘dead time’ where no H_2 evolved from the reactor but where carbon lay-down occurred, indicated that all the hydrogen produced by the thermal decomposition of the fuel was initially

used up by the reduction of the OTM. The OTM's reduction by H_2 was preferential to that by methane or sunflower oil fuel, as would be expected of a conventional Ni-based catalyst. In conditions of low fuel flow, the highest steam conversions once steam reforming had reached a steady level were obtained. These results suggested collectively that an intermediate fuel-only flow step, sandwiched between the airflow and the fuel/steam feed steps, should be beneficial in achieving a quick and necessary OTM reduction without the enthalpic burden of superfluous steam. We therefore show that in the USR process, the oxygen transfer material needs to act as a steam reforming catalyst as well. This could have implications on its claims of insensitivity to catalyst poisons such as sulphur [3-4], which our future work on the USR process will be addressing.

When using sunflower oil as the fuel, ca. 15% of the carbon products ended up as methane, indicating the potential for further H_2 production. When using a mineral dolomite to shift the water-gas reaction to higher H_2 yields, the process showed a high sensitivity to the reactor temperature under fuel/steam flow in the 600-650°C range, a result expected from our preliminary thermodynamic calculations, and in near-agreement with the literature of low partial pressure CO_2 sorption on similar materials. The thermodynamic calculations indicated that it was due to a large drop in carbonation efficiency over a small temperature range (e.g. 93% dry H_2 at 600°C and only 75% at 650°C).

Considerable work remains to be done with regard to the optimisation of the process, in particular achieving conditions of autothermality, for which carbon formation/oxidation and sorbent carbonation/decomposition will be expected to be important enthalpic contributors given the role they played in near-isothermal conditions and our thermodynamic predictions. The USR process

fulfilled its promise of maintaining initial efficiency under heavy coking conditions due to the complete carbon oxidation under each air flow, offering the possibility of using a diverse range of coking fuels for hydrogen production. We hope to conduct investigations of the USR process using other liquid fuels such as low- and high-lignin biomass pyrolysis oils, waste tyres pyrolysis oils, waste cooking oils and industrial/vehicle waste oils in the future in order to study investigate further its claims of fuel flexibility and insensitivity to catalysts poisons.

Acknowledgments

We are grateful to the EPSRC for the grant GR/R50677/01, Dr Phil Ingram at Johnson Matthey, and Andrew Holt at Catal for helpful discussions and materials. Thanks also to Miss E. Knight for experimental assistance in the TGA work.

References

1. K. Vijayaraghavan, M. Amin Mohd Soom. Trends in biological hydrogen production-a review. International Journal of Hydrogen Energy. in press. Available online 23 Dec 2004.

2. F. R. Hawkes, Dinsdale R., D. L. Hawkes, and I. Hussy. International Journal of Hydrogen Energy 27 (2002) 1339-1347.

3. R. V. Kumar; J. A. Cole; R. K. Lyon. Preprints of Symposia, J. Am. Chem. Soc. 1999, 44, (4)

4. Lyon R. K., Cole J. A. *Combustion and Flame*; 121 (2000) 249-261.

5. R. Kumar, C. Moorefield, P. Kulkarni, B. Eiteneer, J. Reinker, V. Zamansky. Autothermal Cyclic Reforming and H_2 refueling system. DOE project review May 2004, Philadelphia.

6. G. Rizeq, J. West, A. Frydman, R. Subia, V. Zamansky, H. Loreth, L. Stonawski, T. Wiltowski, E. Hippo, S. Lalvani. Fuel-Flexible Gasification-Combustion Technology for Production of H_2 and Sequestration-Ready CO_2. Quarterly Technical Progress Report No. 9. January 2003. DOE contract: DE-FC26-00FT40974.

7. V. M. Zamansky. Clean Coal Day in Japan, Tokyo, Japan, Sept 3-4 2002.

8. P. Glarborg, R. J. Kee, J. F. Grcar, J. A. Miller, "PSR: A Fortran Program for Modeling Well-Stirred Reactors", Sandia National Laboratories Report SAND86-8209(86). Version 2.2 (1992 update).

9. J.-W. Snoeck, G. F. Froment and M. Fowles. Ind. Eng. Chem. Res. 41 (2002) 4252-4265

10. D. E. Riddler, M. V. Twigg, in : M. V. Twigg (Ed), Catalyst Handbook 2nd Edition, Wolfe Publishing Ltd, 1989, pp244-250

11. A. B. Ross, V. Dupont, I. Hanley, J. M. Jones, and M. V. Twigg. Clean Air 2003. 7-10th July 2003, Lisbon, Portugal.

12. A. B. Ross, V. Dupont, I. Hanley, J. M. Jones, and M. V. Twigg. Abstracts of papers of the American Chemical Society 228: u676-u676 151-fuel part 1 Aug 22, 2004

13. A.B. Ross, I. Hanley, V. Dupont, J. M. Jones, M. V. Twigg. *Science in thermal and chemical biomass conversion* Vol.1, pp. 444-459. Ed Tony Bridgewater and D.G.B. Boocock. Publ. Antony Rowe Ltd, Chippenham.

14. J.Adanez., F. Garcia-Labiano, L.F. de Diego and V. Fierro. Energy and Fuels 1998, 12, 726-733.

15. M. Olszak-Humienik and J. Mozejko. Journal of Thermal Analysis and Calorimetry, Vol. 56 (1999), 829-833.

16. K. Chrissafis, C. Dagounaki and K.M. Paraskevopoulos. Thermochimica Acta 428 (2005) 193-198.

Tables

Table 1
Thermodynamics equilibrium predictions: comparison USR with CSR/CPO. Rows 1 and 2 are for USR in absence of CO_2 sorbent, rows 3 and 4 are for USR with CO_2 sorbent (MO=CaO), row 5 is for the autothermal steam reforming coupled with partial oxidation.

Process	T (°C)	Reactants 1 mol in	% Conv	% CO_2 sel.	% CO Sel.	% Dry H_2	ΔH in J/mol (reactant)	*H_2 Prod.Eff.	**CO Prod.Eff.
USR-FF- No sorb No $C_{(S)}$	800	0.3040 CH_4 0.4323 H_2O 0.2637 NiO	99.8 30.7 100	30.7	69.3	70.9	2.43×10^5 (NiO)	0.711	0.69
USR-AF no sorb.	800& 1000	2/3Ni 1/3O_2	100 100	n/a	n/a	n/a	-2.40×10^5 (Ni)	n/a	n/a
USR-FF CaO sorb no $C_{(S)}$	717	0.249 CH_4 0.343 H_2O 0.232 NiO 0.088 CaO	98.4 37.5 100 54.7	27.5	52.9	75.5	1.8×10^5 (NiO)	0.81	0.57
USR-AF CaO sorb	1000	0.532 Ni 0.266 O_2 0.202$CaCO_3$	99.8 100 94.8	n/a	n/a	n/a	-1.80×10^5 (Ni)	n/a	n/a
CSR/CPO no $C_{(S)}$	800	0.35 CH_4 0.5 H_2O 0.15 O_2	99.7 31.2 100	30.6	69.4	70.9	0.02×10^5 (CH_4)	0.713	0.69

*H_2 production efficiency ('H_2 Prod.Eff.') is in mol of H_2 output per mol 2H input from all reactants.
**CO Prod. Eff. is in mol of CO output per mol of elemental C input from all reactants. The latter is of interest for syngas production.

Table 2.
Ni-based OTM's composition (increasing Ni content), thermal stability from TGA, Max. rates of O_2 and Ni conversion

OTM	Wt% Ni	Balance	TGA: Wt% loss @ 1000°C	Max rate of O_2 conv. (% s^{-1})	Max. rate of Ni oxid. (% s^{-1})
B	12.6	alumina	0.25	14.8	10.6
D	14.1	support	7.8	13.7	8.3
E	20	support	0.0	12.3	6.2
A	27.5	4wt% MgO	0.7	12.5	3.9
C	39.2	8wt % CaO	0.2	19.0	9.5

Table 3
Summary of results obtained for various OTMs in the reconfigured bench scale USR-FF using N_2-diluted steam/CH_4 ratio of 1.8 at 800°C in absence of CO_2-sorbent, the mass of OTM is 40g for all experiments reported in the table.

OTM	Ni Wt%	V_{CH4} sccm	Dead Time ratio	Avg % Conv CH_4	Avg % Conv H_2O	Avg %Sel. CO_2	Avg %Sel. CO	Avg %Sel $C_{(S)}$	Avg corr. dry*%H_2	Avg. H_2 Prod.Eff	Final H_2 Eff
B	12.6	152	1/2	99.0	51.3	26.1	68.5	5.4	75.4	0.764	0.41
A	27.5	152	1/3	98.2	47.3	25.6	68.8	5.6	74.5	0.725	0.51
C	39.2	152	2/3	98.9	28.9	29.0	64.2	6.8	72.8	0.658	0.28
B	12.6	400	1/6	98.8	39.4	17.5	68.1	14.4	75.8	0.706	0.62
A	27.5	400	1/6	98.9	38.0	16.5	70.5	13.0	75.5	0.700	0.62
C	39.2	400	1/6	99.1	36.7	15.9	70.3	13.8	75.6	0.695	0.59

Average values are only over the period of established steam reforming . Duration of FF is 600 s. 'Dead Time ratio' indicates the fraction of the duration of the FF for which initially no H_2 leaves the reactor. Dry H_2 content has been corrected for zero N_2 content. Final H_2 efficiency is total hydrogen converted from CH_4 and H_2O by the end of the FF step.

Table 4
Summary of results obtained for OTM 'A' during the bench scale USR tests using sunflower oil with N_2-diluted steam/C ratio of 1.8 in the absence of CO_2-sorbent over a bed of 80 g of OTM at 700°C. As previously, average reported values are over the period of established steam reforming. Headings are defined as in Table 3. The duration of the FF step was 400 s. Sunflower oil molar composition: $C_{18}H_{34.4}O_{2.1}$.

OTM	*Oil Liq. Flow cm^3/min	Oil Molar in Flow Mol/s	Dead Time	%Conv oil	%Conv H_2O	%Sel. CO_2	%Sel. CO	%Sel. CH_4	%Sel. C(S)	% corr. dry H_2	H_2 Prod. Eff.	Final H_2 Eff
A	0.575	3.1×10^{-5}	1/4	100	32	36.6	7.9	15.5	39.9	67.2	0.44	0.37

Figure legends

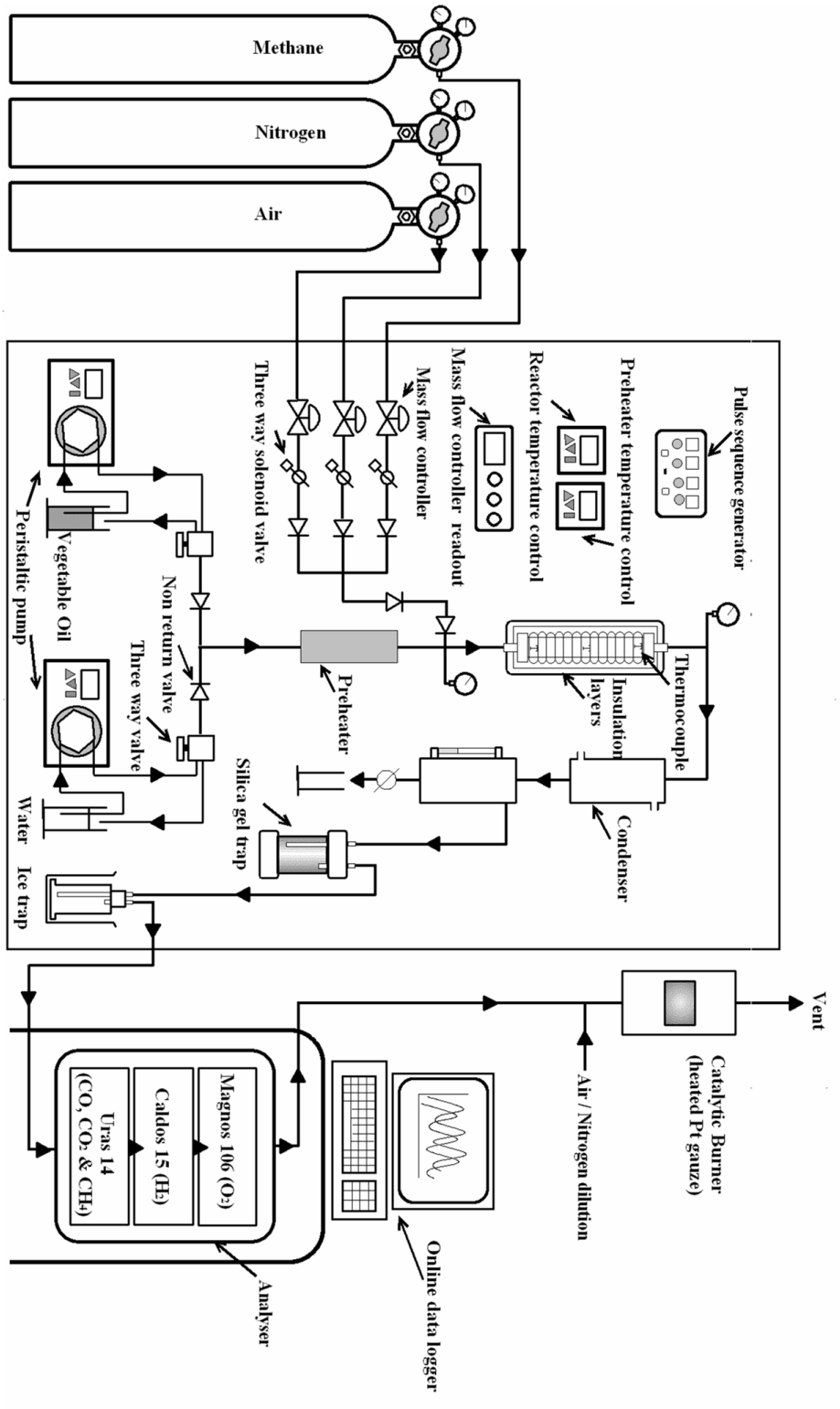

Fig. 1 Schematic of the bench-scale unmixed steam reforming set-up.

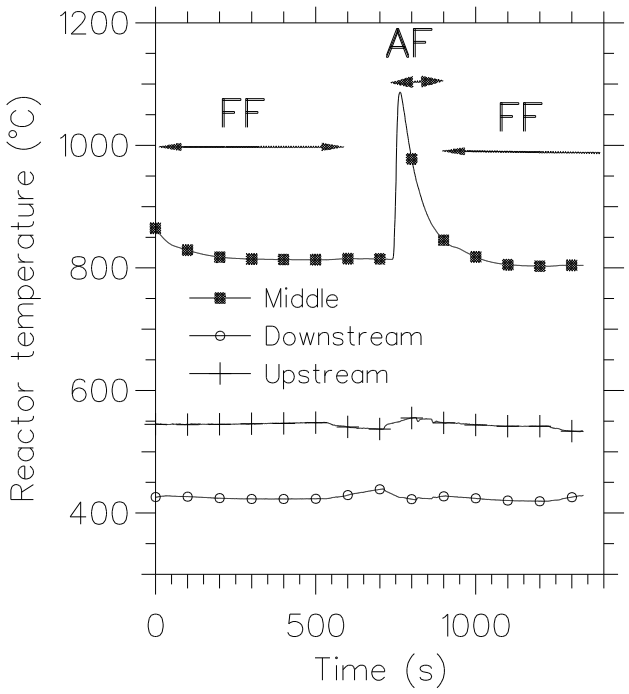

Fig. 2 Typical temperature histories during the bench scale near isothermal USR tests.

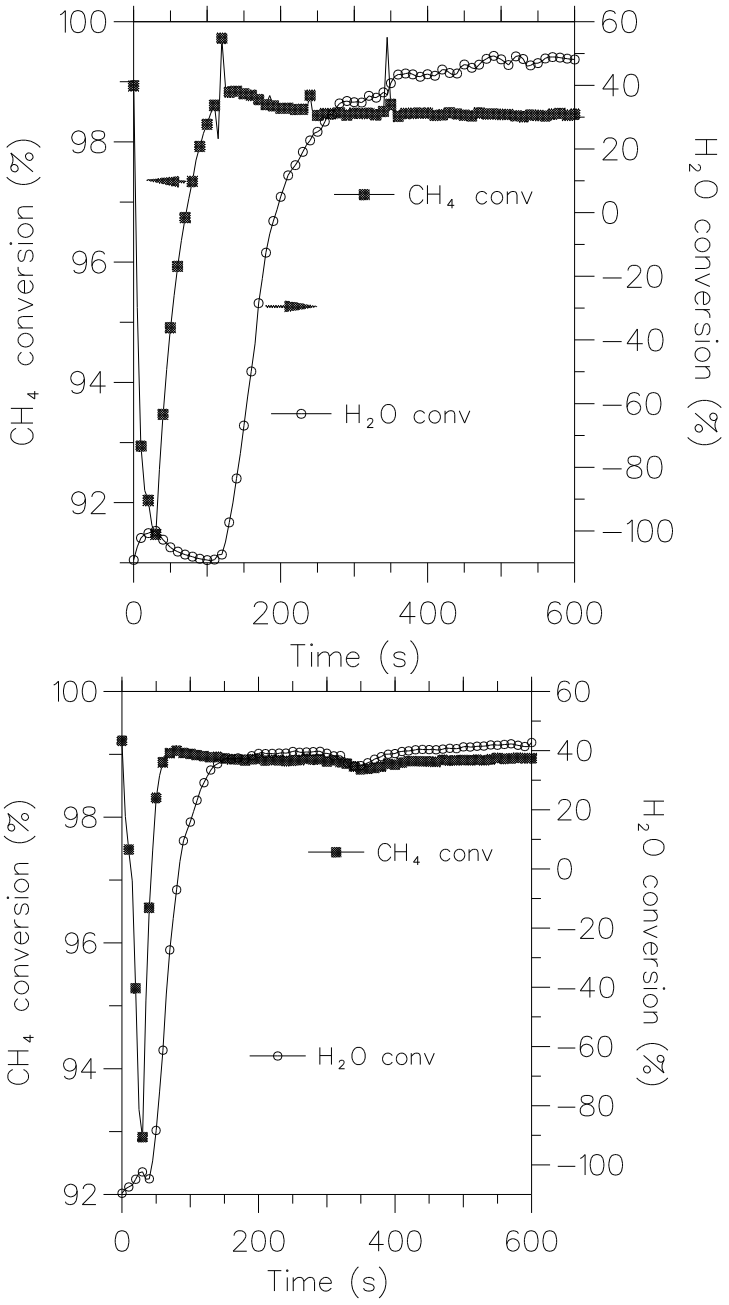

Figs. 3a-b Methane and steam percent conversions during FF on 40g of OTM 'A' for a reactor set temperature of 800°C, steam/methane molar ratio of 1.8 using a step duration of 600 s (a) methane flow of 152 sccm (1.13×10^{-4} mol of C /s) and (b) 400 sccm (3×10^{-4} mol of C /s).

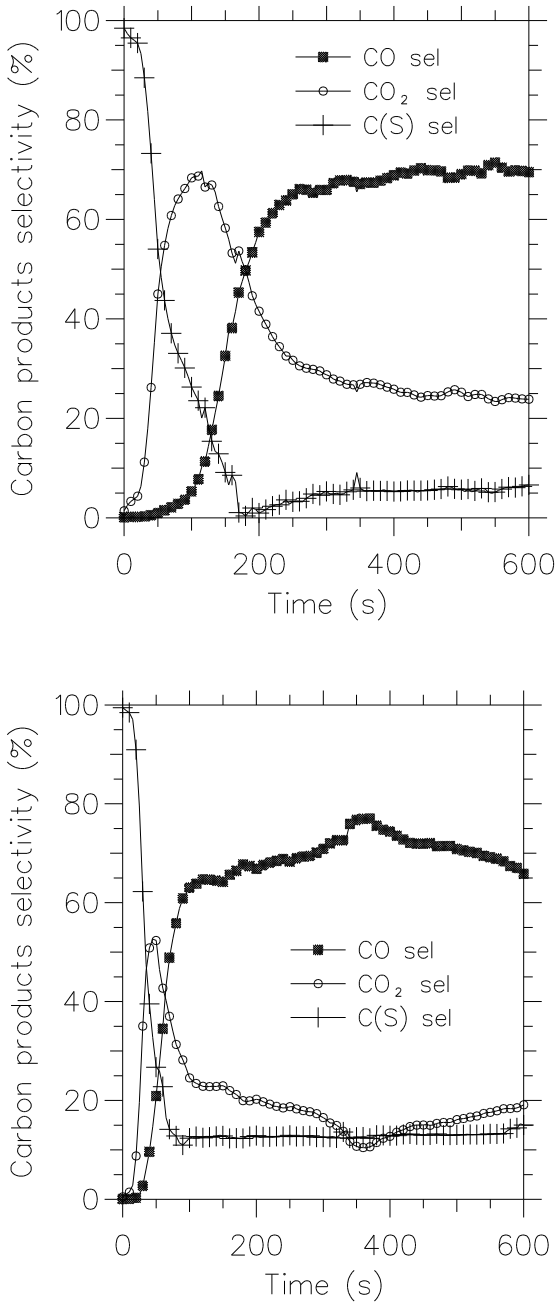

Figs. 4a-b Selectivity of CO, CO_2 and C(S). Same conditions as Figs. 3a-b

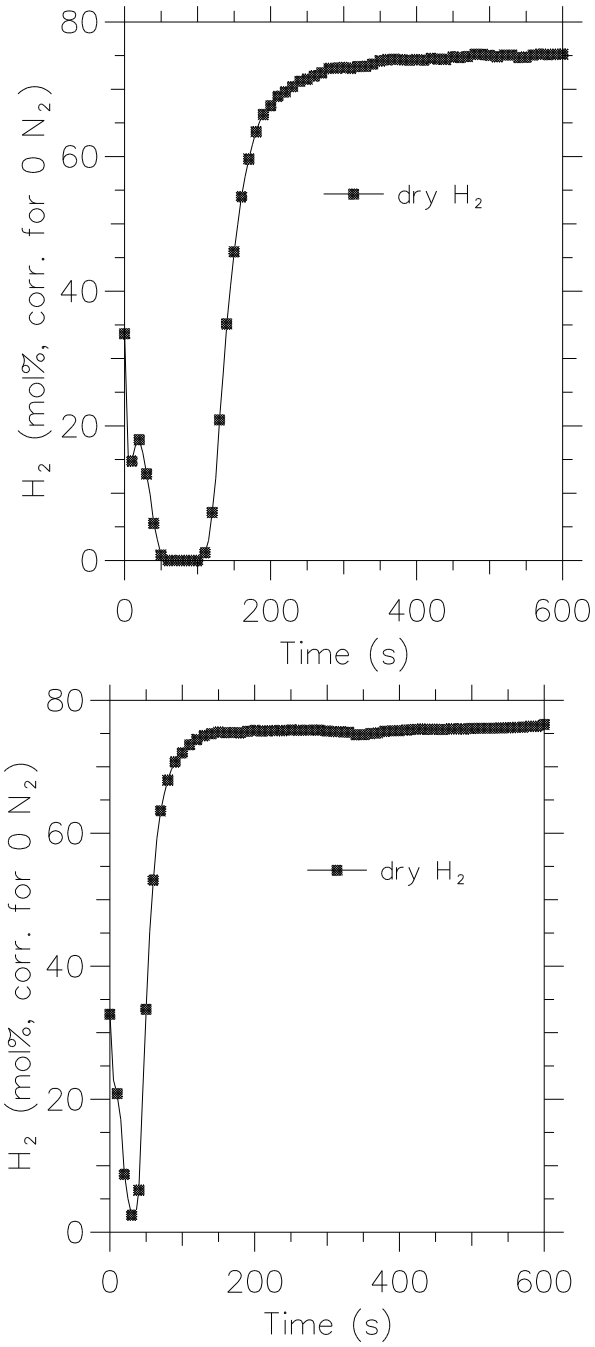

Figs. 5a-b H_2 content in reactors' gas effluents on a dry basis and corrected for zero N_2. Same conditions as Figs. 3a-b.

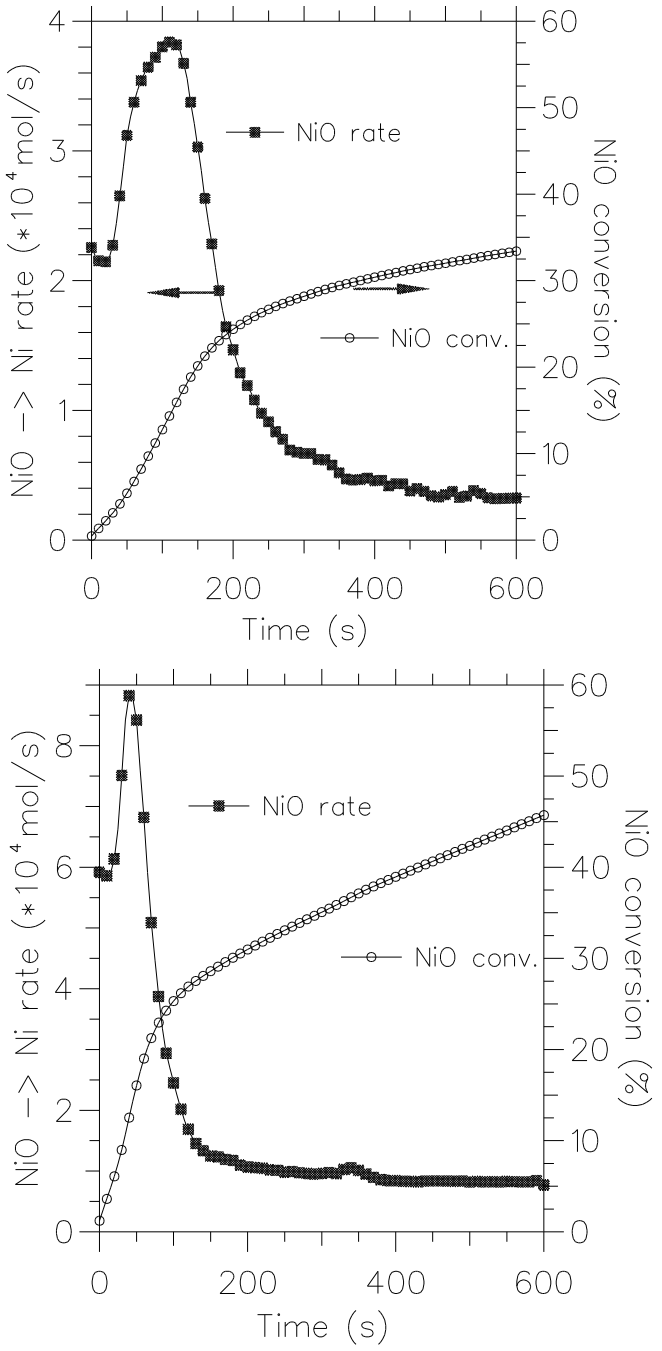

Figs. 6a-b NiO rate of conversion (mol/s) and NiO conversion (% of total Ni in reactor). Same conditions as in Figs. 3a-b.

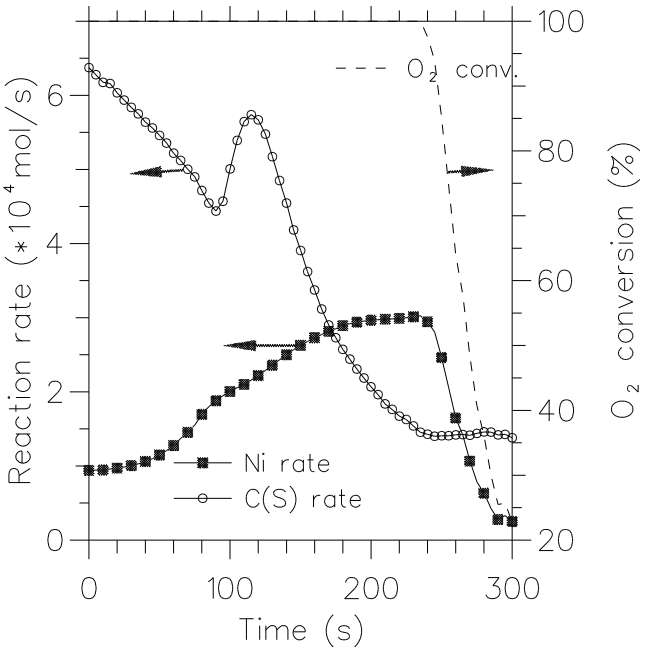

Fig. 7 $C_{(S)}$ and Ni oxidation rates (mol/s) and O_2 conversion (%) during AF step (1200 sccm of air) following a sunflower oil/steam step on 80g of OTM 'A' (reactor set temperature of 700°C, peaks to 1000°C).

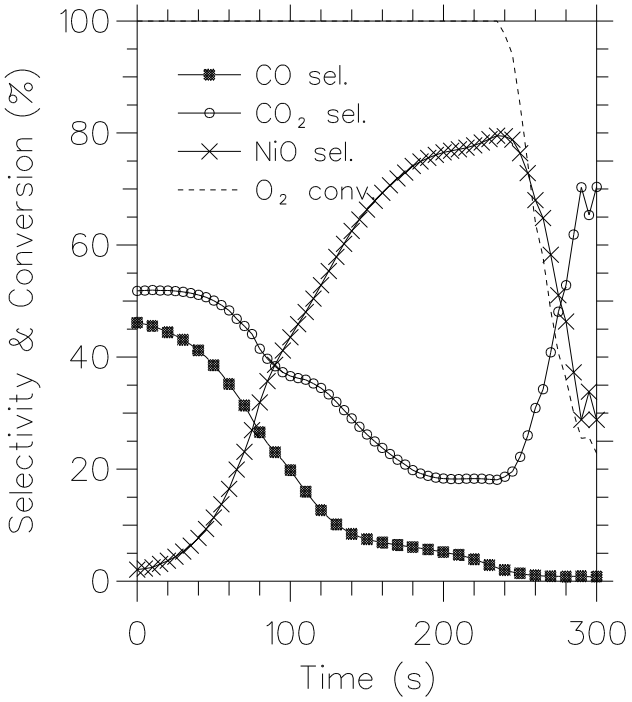

Fig. 8 Selectivity of CO, CO_2 and NiO, and O_2 conversion (%) in the same conditions as in Fig. 7.

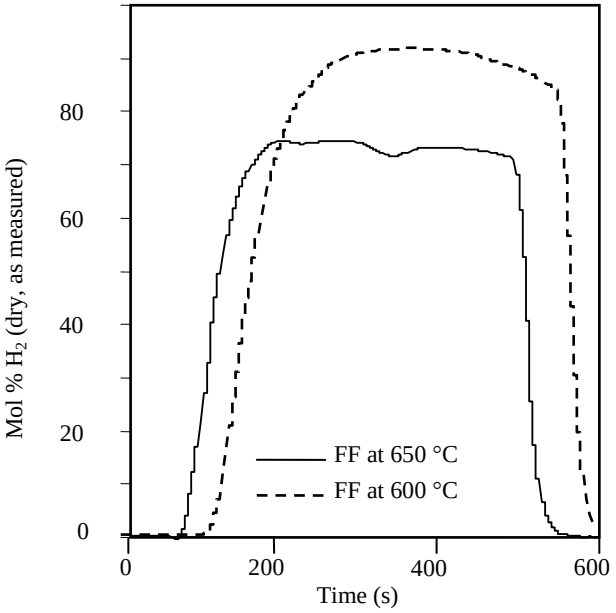

Fig. 9 H_2 content in reactor's gas effluents on a dry basis when using a reactor set temperature of 600°C (dashed line) and 650°C (solid line) during FF step, over 64 g of OTM 'A' and 21 g of dolomite homogeneously mixed. The flow of methane was maintained at 200 sccm, with a steam to carbon ratio of 4.

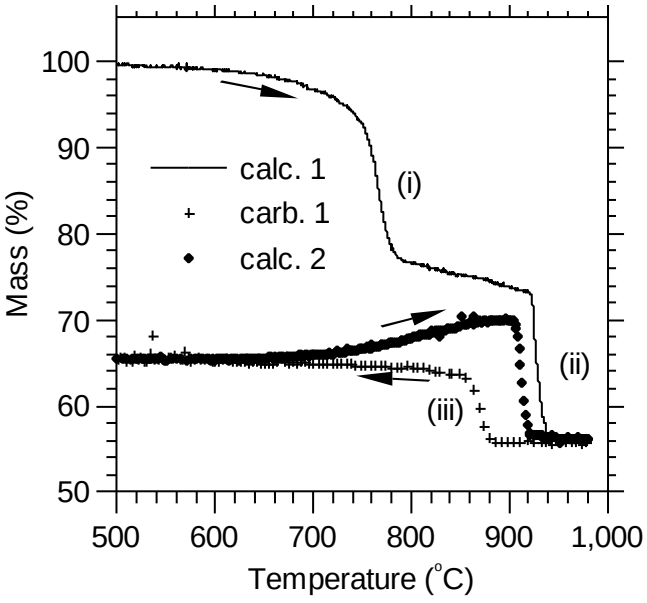

Fig. 10 Thermal decomposition-carbonation-second thermal decomposition cycle of the Sierra de Arcos dolomite. (i) is $CaMg(CO_3)_2 \rightarrow CaCO_3 + MgO + CO_2$ (ii) is $CaCO_3 \rightarrow CaO + CO_2$, (iii) is $CaO + CO_2 \rightarrow CaCO_3$ (MgO does not re-carbonate).